Planar fluidic channels on TiO_2 nanoparticle coated paperboard

Dimitar Valtakari, Milena Stepien, Janne Haapanen, Hannu Teisala, Mikko Tuominen, Jurkka Kuusipalo, Jyrki M. Mäkelä, Martti Toivakka, and Jarkko J. Saarinen

KEYWORDS: Wetting, TiO_2, Nanoparticle, Fluidic channel, Liquid flame spray, Paperboard

SUMMARY: A new design for permanent, low-cost, and planar fluidic channels on TiO_2 nanoparticle coated paperboard is demonstrated. Initially superhydrophobic TiO_2 nanoparticle coatings can be converted to hydrophilic by ultraviolet (UVA) light, and fluidic channels can be generated. A simple water treatment after the UVA illumination converts the channels permanent when nanoparticles are removed from the illuminated and wetted areas as shown by water contact angle, FE-SEM, XPS, and ToF-SIMS analysis. This suggests new routes for inexpensive, easy to use point-of-care diagnostics based on planar fluidic channels.

ADDRESSES OF THE AUTHORS:
Dimitar Valtakari[1] (dimitar.valtakari@abo.fi)
Milena Stepien[2] (stepienm@agh.edu.pl)
Janne Haapanen[3] (janne.haapanen@tut.fi)
Hannu Teisala[4] (hannu.teisala@tut.fi)
Mikko Tuominen[5] (mikko.tuominen@sp.se),
Jurkka Kuusipalo[4] (jurkka.kuusipalo@tut.fi)
Jyrki M. Mäkelä[3] (jyrki.makela@tut.fi)
Martti Toivakka[1] (martti.toivakka@abo.fi)
Jarkko J. Saarinen[1] (jarkko.j.saarinen@abo.fi)

[1]Abo Akademi University, Laboratory of Paper Coating and Converting, Center for Functional Materials at Biological Interfaces (FUNMAT), Porthansgatan 3, FI-20500 Åbo/Turku, Finland

[2]AGH University of Science and Technology, Academic Centre for Materials and Nanotechnology, al. A. Mickiewicza 30, 30-059 Krakow, Poland

[3]Tampere University of Technology, Aerosol Physics Laboratory, Department of Physics, P.O. Box 692, FI-33101 Tampere, Finland

[4]Tampere University of Technology, Paper Converting and Packaging Technology, Department of Materials Science, Tampere University of Technology, P.O. Box 589, FI-33101 Tampere, Finland

[5]SP Technical Research Institute of Sweden, P.O. Box 857, SE-50115 Borås, Sweden

Corresponding author: Jarkko J. Saarinen

Cellulose is the most abundant natural biopolymer on Earth. Traditionally cellulose fibres have been used in different paper products from newspapers and magazines to packaging applications from paperboard boxes to wrapping papers. Recently, functional applications on paper-based substrates have raised interest as they provide both economically and ecologically sustainable alternatives for fossil fuel based plastic substrates. Microfluidic devices (Martinez et al. 2008; Fobel et al. 2014; Songok et al. 2014), bioactive paper (Pelton 2009), sensors (Sarfraz et al. 2012), transistors (Bollström et al. 2009), displays (Siegel 2009), photovoltaics (Barr et al. 2011; Hübler et al. 2011), and paper-based electronics (Tobjörk, Österbacka 2011) have been demonstrated within the past decade. Recyclability is especially important for reducing the environmental burden of electronic waste (Irimia-Vladu et al. 2012) with the expected exponential growth of the internet of things utilizing printed and thin electronic structures on flexible substrates.

Wetting plays an important role in e.g. printing, coating, painting, and laminating. Conventionally surface wettability of paper is controlled by surface sizing using either alkylketene dimer (AKD) or alkenyl succinic acid (ASA) that reduce the surface wetting of pure cellulose substrates (Hubbe 2007). Microfluidic devices and channels have typically been fabricated on a glass or polymer substrate using microelectronics tools such as photolithography and etching (Whitesides 2006). On paper different strategies for forming the patterned structures have been taken: for example, wax has been used as a barrier, hydrophobic material for formation of microfluidic paper-based analytical devices (Martinez et al. 2010; Vella et al. 2012) or alternatively a thin plasma coating of a fluorocarbon film has been utilized (Balu et al. 2008).

We have recently shown that TiO_2 nanoparticles on a paperboard surface results in a superhydrophobic surface due to a carbonaceous layer on top of the nanoparticles (Teisala et al. 2013) originating from the volatile organic compounds emitted during the flame deposition whereas SiO_2 nanoparticles resulted in a highly hydrophilic surface (Stepien et al. 2011). The nanoparticle coatings were deposited by a liquid flame spray (LFS) process (Mäkelä et al. 2011). It is worth emphasizing here that both TiO_2 and SiO_2 exhibit superhydrophilicity as pure thin films (water contact angle ~ 0°) (Takeda et al. 1999) and TiO_2 superhydrophobicity is only observed on paperboard substrate (Aromaa et al. 2012) due to volatile organic compounds originating from the base paper pigment coating.

LFS is a cost-effective way to deposit various metal and metal oxide nanoparticles on large area via roll-to-roll process flow at atmospheric conditions. Web speeds exceeding 150 m/min can be achieved allowing several m^2 of nanoparticle coated surfaces to be manufactured in a minute with a single burner nozzle. In LFS an organometallic liquid precursor typically dissolved in isopropyl alcohol (IPA) is fed into a high velocity and high temperature H_2-O_2 flame in which the precursor evaporates, reacts, nucleates, and forms solid nanoparticles that can be collected on various substrates from glass and steel to paper and plastic films (Mäkelä et

al. 2006). The relatively narrow size distribution and sizes of nanoparticles can be controlled from 2 to 200 nm simply by changing the deposition parameters i.e. the relative gas flows, the precursor feed rate and concentration, and the distance of the nozzle from the deposited surface (Mäkelä et al. 2004). LFS has been used for glass coloring (Gross et al. 1999), catalytic applications (Keskinen et al. 2006), and antibacterial surfaces (Gunawan et al. 2009).

Well-known photocatalytic properties of TiO_2 (Fujishima et al. 2000) can be used to convert the TiO_2 nanoparticle coated paperboard surface from superhydrophobic to a highly hydrophilic one under ultraviolet (UVA) light, and different patterns can be formed using a photomask. The changes in the wettability correlate well with the changes observed in the surface chemistry using an X-ray photoelectron spectroscopy (XPS) (Stepien et al. 2012) and time-of-flight secondary ion mass spectrometry (ToF-SIMS) (Stepien et al. 2013). However, the achieved wettability conversion is reversible i.e. the recovery of surface hydrophobicity occurs under ambient conditions in dark during storage, and the change can be accelerated by heat.

In this paper we show, for the first time to our knowledge, the fabrication of permanent planar fluidic channels on such TiO_2 nanoparticle coated paperboard using a simple water treatment of the UVA illuminated, photocatalytically converted channels. The illuminated wetting channels are exposed to water that transports the nanoparticles to the channel edges and deeper into the base paperboard resulting in a permanently less hydrophobic channel. The changes in the channel morphology are measured using a field emission scanning electron microscope (FE-SEM), contact angle (CA), XPS, and ToF-SIMS. A similar wetting approach was previously taken with randomly roughened polymethylmethacrylate (PMMA) substrates to stabilize the nanotextured surface before its hydrophobization (Gnanappa et al. 2012). The current set-up avoids all problems with surface recovery during the storage and has thus a high potential, for example, in cost-effective, disposable point-of-care (POC) type diagnostics. An additional benefit of cellulose is easy disposability by combustion after such an analysis leaving no hazardous biological waste.

Materials and Methods

Sample preparation

The paperboard substrate for the TiO_2 LFS nanoparticle deposition was a commercial, online double pigment coated paperboard (200 g/m^2, Stora Enso, Sweden). The LFS deposition process is schematically shown in *Fig 1a*. TiO_2 nanoparticles were deposited in an atmospheric roll-to-roll process using the coating and laminating pilot line at the Tampere University of Technology (Tampere, Finland) with a constant web speed of 50 m/min. Titanium (IV) isopropoxide (TTIP; 97% pure, Aldrich, St. Louis, MO, USA) dissolved in isopropyl alcohol (IPA) precursor with a metal ion concentration of 50.0 mg/ml was used for the TiO_2 nanoparticle coatings. The precursor feeding rate into a spray nozzle was set to 12.0 ml/min located at 6 cm distance from the moving paperboard web. The combustion gases for the process were H_2 (50 l/min) and O_2 (15 l/min).

The 1 and 2 mm wide channel structures were formed using a photomask exposed to the UVA light (Bluepoint 4 ecocure, Hönle UV Technology, Gräfelfing, Germany) having a 365 nm central wavelength under a passband filter for 320 - 390 nm. A schematic of the set-up is presented in *Fig1b*. The exposure intensity was kept constant at 50 mW/cm^2, and the exposure time was 30 min. Our previous results (Stepien et al. 2012) have shown that 30 min UVA exposure converts the initially superhydrophobic TiO_2 nanoparticle coated surface to a highly hydrophilic one. However, the induced hydrophilicity is not permanent, and the superhydrophobicity recovery can be enhanced by a heat treatment in an oven at 150°C for 3 min. To make the channel structure permanent, the UVA illuminated channel area was exposed to water in the first stage wetting as shown in *Fig 2*.

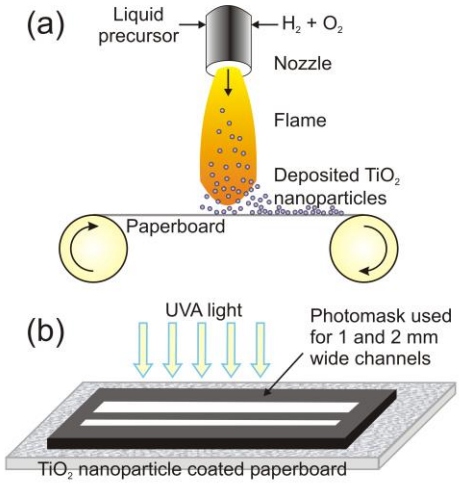

Fig 1 - (a) A schematic of the LFS process used for TiO_2 nanoparticle deposition and (b) the UVA light activation of the 1 and 2 mm wide planar channel structures on TiO_2 nanoparticle coated paperboard.

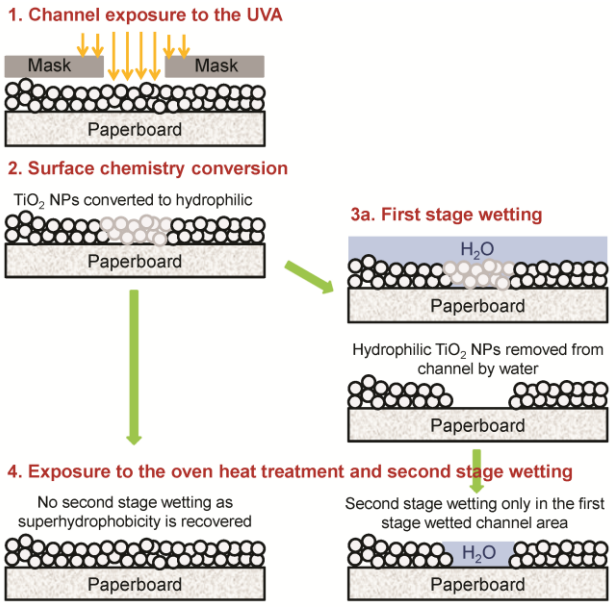

Fig 2 - A schematic of the sample preparation using a two-stage wetting process with the UVA illuminated channel structures.

The TiO_2 nanoparticles are removed from the hydrophilic channel area during the first stage wetting. Both UVA illuminated samples (with and without the first stage wetting) were finally heat treated in an oven at 150°C for 3 min. Without the first stage wetting the TiO_2 nanoparticles remain on the surface and convert back to superhydrophobic surface in an oven heat treatment whereas the second stage wetting only occurs in the first stage wetted channel. Both samples were kept at 24°C and at a relative humidity of 50% overnight after the oven heat treatment before the measurements.

Sample characterization

Water contact angles (CAs) were measured using a sessile droplet method with a contact angle goniometer (KSV CAM 200, Biolin Scientific, Finland) with a droplet volume of approximately 6 µl. The CA measurements were carried out over an illuminated, first stage wetted and oven heated area of 1×1 cm^2 that is used to guarantee adequate water droplet setting without the boundary effects. A single water droplet was used in the center of such square, three parallel measurements were performed. The samples were imaged using a field emission scanning electron microscope (FE-SEM; Zeiss LEO Gemini 1530, Germany) with an in-lens detector. The samples were carbon coated prior to imaging for conductivity. Topographical imaging was carried out using the secondary electron (SE) imaging mode with a magnification of ×50,000 and ×5,000 with an accelerating voltage of 2.70 kV and a working distance of 4 to 5 mm.

To study the surface chemistry of the channel structures X-ray photoelectron spectroscopy (XPS) measurements were carried out using a PHI Quantum 2000 instrument (Physical Electronics Instruments, USA) with a monochromatic Al Kα X-ray source operated at 25 W. XPS is sensitive approximately 10 nm depth into the surface. Charge compensation was improved by a combination of electron flood and ion bombarding. Take-off angle of 45° relative to sample surface was used. High-resolution photoemission peaks for C 1s, O 1s, and Ti 2p were measured from three different spots using a pass energy of 29.35 eV. A mixed Gaussian– Lorentzian fit and Shirley background reduction were used for curve fitting. The main chamber pressure was kept at 2×10^{-7} Torr during the measurement.

For a more detailed surface chemical characterization from 1-2 nm from the sample surface, a time-of-flight secondary ion mass spectroscopy (ToF-SIMS) was used. ToF-SIMS spectra were acquired using a PHI TRIFT II (USA) unit with a pulsed liquid metal ion gun. Positive ion mode over the mass range of 2 − 2000 Dalton (Da) was used with a Ga+ primary source having a 100×100 μm^2 raster size, a 15 kV applied voltage, a 600 pA aperture current, and a 10 min acquisition time. Sample surface charging was reduced by using a low electron energy flood gun. A noninterlaced mode (the analysis and sputtering are active in different ToF cycles) was used for image collection from an area of 2 × 2 mm^2. At least three different spots on each sample were measured.

Results and Discussion

Fig 3 presents a comparison of 1 and 2 mm wide channel structures with and without the first stage wetting step. *Fig 3a* shows the non-wetted channel that is exposed to red colour stained (Amaranth dye) water. However, no channel structure is visible with water droplets not able to adhere on the tilted surface as the UVA illuminated channel area shown by yellow lines recovers the initial superhydrophobicity by the oven heat treatment, and thus the channel structure is lost. On contrary, *Fig 3b* shows a clear second stage wetting in the channel structures on the first stage wetted sample.

Table 1 summarizes the measured water contact angles of the TiO_2 nanoparticle coated paperboard as prepared (CA ~ 160°), and after the UVA illumination (CA ~ 5°), heat treated first stage wetted channel (CA ~ 110°), and a post UVA illumination (CA ~ 65°). We have shown before (Stepien et al. 2012) that the heat treatment results in a recovery of the initial superhydrophobic surface with CA of approximately 150°. In *Table 1* the CA of the first stage wetted channel is close to 110° after the heat treatment that is significantly lower than the initial superhydrophobic value. Therefore, the channel structure has permanently higher wettability than without the first stage wetting.

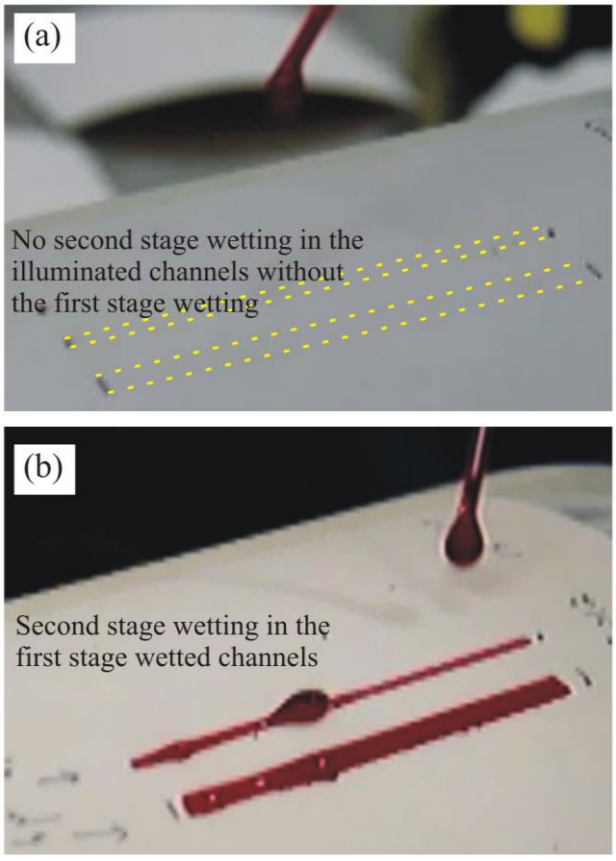

Fig 3 - Images of wetting behaviour of samples without (a) and with (b) the first stage wetting in 1 and 2 mm wide channel structures that are exposed to red colour stained water. The illuminated channels are shown by yellow dotted lines in (a) that are converted back to superhydrophobic by the heat treatment with no wetting by the coloured water.

Table 1 - Water contact angles of the channel area

Sample	CA
Reference base paperboard	78°
Initial TiO_2 NP surface	160°
UVA illuminated channel	5°
Heat treated first stage wetted channel (0 s)	110°
Heat treated first stage wetted channel (60 s)	100°
Heat treated first stage wetted channel exposed to post UVA illumination (0 s)	102°
Heat treated first stage wetted channel exposed to post UVA illumination (60 s)	65°

Table 2 - Relative amounts of elements in different elements.

Sample	C 1s	O 1s	Ti 2p
Reference base paperboard	54.8	35.4	-
First stage wetted / channel	55.1	35.4	9.1
First stage wetted / outside	49.0	38.8	12.2
Non-wetted / channel	51.4	36.8	11.0
Non-wetted / outside	48.9	38.5	12.6

Furthermore, the initial CA of 110° will decrease to 100° within 60 seconds. A secondary post-UVA illumination of the channel area reduces the CA to 102° that will settle into 65° within 60 seconds. This value is close to the reference base paperboard CA value of 78°. Hence, this suggests that the amount of TiO_2 nanoparticles is significantly reduced in the first stage wetted channel as the channel does neither reach the initial superhydrophobicity nor the high hydrophilicity after the secondary UVA treatment. In both cases a permanent channel is formed in which water droplets will locate and adhere to.

Electron microscopy was used to confirm the nanoparticle reduction hypothesis. *Fig 4* shows the FE-SEM and ToF-SIMS total ion count images of the UVA and heat treated channels. The first stage wetted channel is displayed on the left-hand side with a significant difference compared to non-wetted channel structure on the right-hand side image. The width of the channel structure corresponds well to the used UVA photomask with an exposure width of 1 mm. The main mechanism for the LFS deposited nanoparticle adhesion to the surface is by van der Waals forces i.e. the particles are loosely bound to the surface. Therefore, water wets the channel area (CA < 10°) in the first stage, and the nanoparticles are transported from the channel area along the moving liquid contact line, pushed to the edges similar to the coffee stain effect (Deegan et al. 1997), or absorbed deeper into the base paperboard mineral pigment coating. A significant difference is also observed in the ToF-SIMS total ion count spectra: the first stage wetted channel is clearly visible after the heat treatment with a reduced total ion count in the channel (the red area).

The surface morphology was studied in a more detail using an FE-SEM imaging. *Fig 5* displays the high magnification images of the channel and edge region of the first stage wetted channel area in comparison to the reference base paperboard. The area outside the channel (no UVA exposure, oven heat treatment only) in *Fig 5a* shows a typical morphology of the LFS deposited TiO_2

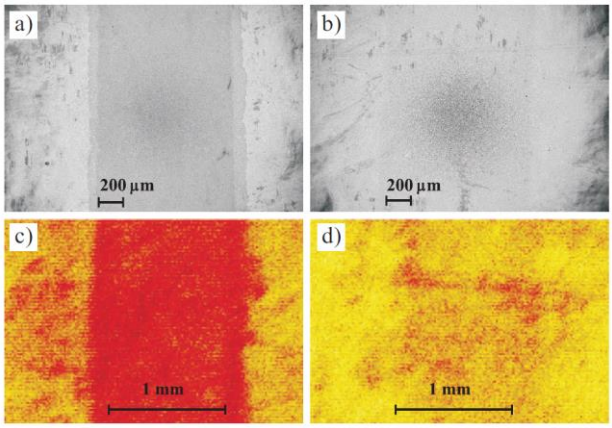

Fig 4 - FE-SEM (a,b) and ToF-SIMS images of total ion counts in positive ion mode (c,d) of the channel structure with (left) and without (right) the first stage wetting in a 1 mm wide channel structure.

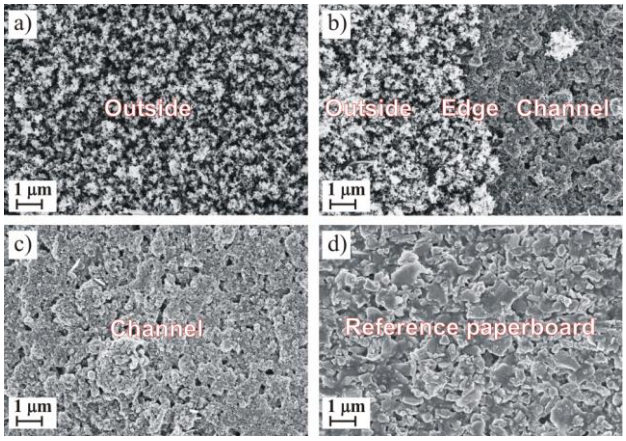

Fig 5 - FE-SEM images of outside (a), edge (b), and channel (c) areas of the first stage wetted TiO_2 nanoparticle coated surface compared to a reference pigment coated base paperboard (d). A rosette like structure of TiO_2 nanoparticles fully covering the surface is shown on (a) whereas a typical base paperboard mineral pigment coating structure is clearly visible in the first stage wetted channel (c) with the reduction of TiO_2 nanoparticles resulting in a surface similar to the base paperboard (d).

nanoparticles as observed in our earlier work (Stepien et al. 2013). *Fig 5b* shows the edge area in which a distinct boundary can be observed between the non-illuminated and UVA illuminated, first stage wetted areas. Finally, in the first stage wetted channel a significant decrease in the amount of nanoparticles is clearly visible in *Fig 5c* displaying a typical porous surface morphology of base paperboard mineral pigment coating shown in *Fig 5d*.

The XPS study confirms the observations in the FE-SEM images and the ToF-SIMS mapping. The elemental composition of the surface is displayed in *Table 2*. The reference pigment coated base paperboard does not have any titanium on the surface as expected without TiO_2 nanoparticle coating. The amount of TiO_2 is reduced after the first stage wetting that supports the findings from the FE-SEM images with reduced amount of nanoparticles. Secondly, both carbon and oxygen values are similar to the reference base paperboard. Furthermore, in both samples the outside areas, which are only exposed to the

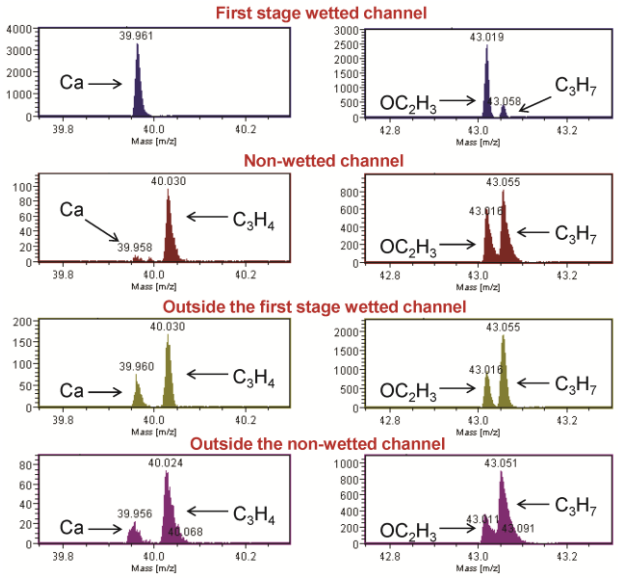

Fig 6 - High resolution ToF-SIMS spectra of peaks 40 and 43 of the different samples

oven heat treatment, have similar values as expected. The slightly reduced amount of titanium in the non-wetted channel area (UVA + oven treatment) can be explained with the increased amount of carbon: the volatile organic components are evaporated in an oven from the base paperboard pigment coating and adhered on top of the TiO_2 nanoparticles as we have also seen in our previous studies (Teisala et al. 2013). A more significant reduction is observed after the first stage wetting that is also in agreement with our previous results (Stepien et al. 2012; Stepien et al. 2013).

The high resolution ToF-SIMS spectra in *Fig. 6* show two different *m*/*z* ranges that correspond to fragments of Ca and C_3H_4 peaks (39.8 − 40.2), and OC_2H_3 and C_3H_7 (42.8 − 43.2). A large Ca-ion peak is only observed in the first stage wetted channel. This correlates well with the XPS measurement of the reference paperboard that has 3.0% relative amount of calcium whereas TiO_2 nanoparticle coated paperboard does not have any calcium present on the surface. The used Millipore water has a pH of 5.6 and in acidic conditions the calcium carbonate in the base paperboard pigment coating starts to dissociate. Hence, as seen from the high resolution FE-SEM image in *Fig 5*, the base paperboard $CaCO_3$ particles in the pigment coating are partially dissociated. We have previously shown that the LFS deposited TiO_2 nanoparticles have a carbonaceous layer on top (Teisala et al. 2013) that results from the volatile organic compounds emitted during the flame deposition from the organic binder material used in the base paperboard pigment coating formulation. Such hydrocarbon layer is also visible in *Fig. 6* as there is no C_3H_4 peak present in the first stage wetted channel at 40.03 as the TiO_2 nanoparticles are removed from the surface within the detection range of the ToF-SIMS.

Fig 6 shows also the high resolution ToF-SIMS spectra of hydrocarbon peaks in the vicinity of *m*/*z* = 43. In the first stage wetted channel a significant increase in the polar oxygenated hydrocarbon peak of OC_2H_3 is observed whereas the non-polar hydrocarbon peak of C_3H_7 is smaller than in the other spectra. The observed chemical changes partially explain the observed differences in wettability. In addition, the changes in the surface morphology caused by the removal of nanoparticles seen in Fig 5 also contribute to the changes in wettability.

We have also recorded high resolution spectra of peaks 54 (SiC_2H_2 and C_4H_6), 55 (AlCO, OC_3H_3, and C_4H_7), 56 (AlSiH, OC_3H_4, and C_4H_8), and 57 ($AlSiH_2$, OC_3H_5, and C_4H_9) confirming that the base paperboard pigment coating color components are only visible in the first stage wetted channel area. It is worth emphasizing here that the ToF-SIMS measurement is surface sensitive to the top 1 - 2 nm i.e. only the outermost molecular layers of the surface are characterized. Therefore, in the non-wetted channel area the ToF-SIMS signal mainly originates from the porous TiO_2 nanoparticle coating layer and the base paperboard is located below the detection range of the ToF-SIMS signal. However, in the first stage wetted channel the base paperboard pigment coating is exposed for ToF-SIMS signal detection that is also supported by the FE-SEM analysis shown in *Fig 5*.

Fig 7 shows the normalized relative intensities of the ToF-SIMS spectra from the channel area of the first stage wetted and non-wetted samples.

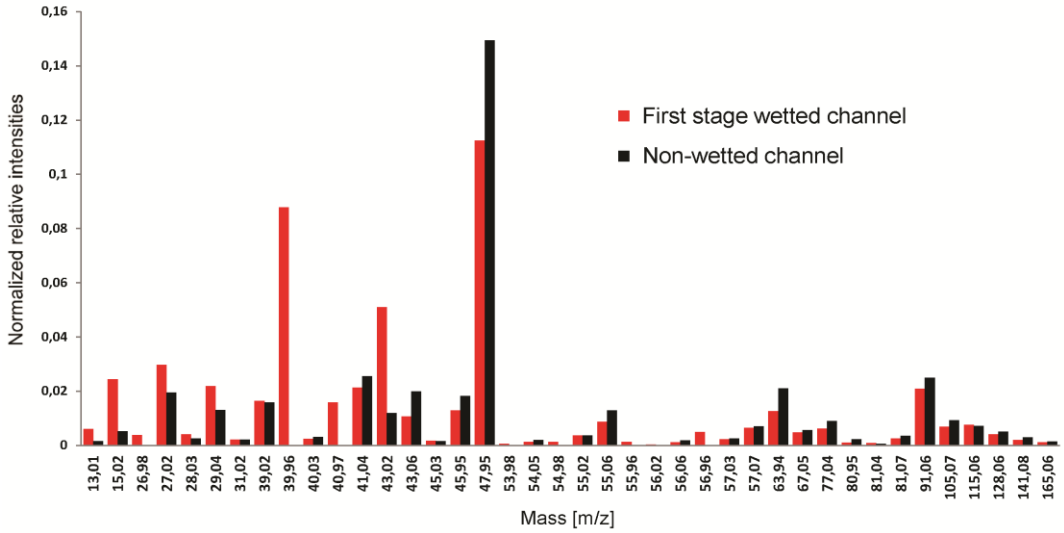

Fig 7 - ToF-SIMS normalized relative intensities for selected peaks in the channel area.

The first stage wetting induces reduction of TiO_2 nanoparticles that is seen in smaller intensities for the peaks *m*/*z* = 45.95 Da (Ti), 47.95 Da (Ti), 63.94 Da (TiO), and 81.07 Da (TiO_2). Furthermore, the peaks related to Al (26.98 Da), Ca (39.96 Da), SiCH (40.97 Da), and $AlSiH_2$ (56.96 Da) are only visible in the first stage wetted spectrum. These peaks are related to the base paperboard pigment coating formulation consisting of kaolin clay. Furthermore, the first stage wetted channel has stronger peaks related to oxygen containing molecules such as peaks CHO (29.04 Da) and C_2H_3O (43.02 Da). Similarly the non-wetted channel shows stronger peaks related to hydrocarbons such as C_3H_5 (41.04 Da), C_3H_7 (43.06 Da), C_4H_7 (55.06 Da), and the peaks between 91.06 - 165.06 Da that originate from the organic binder used in the pigment coating as we have shown in our earlier work (Stepien et al. 2013).

The ToF-SIMS positive ion spectra were also recorded from the areas outside the channel. As expected, the first stage wetted and non-wetted samples are similar in their spectra as the water treatment only affects the channel area in the first stage wetting. The kaolin clay components are not visible in both samples as expected. Small differences were observed in the peaks related to Ti (45.95 and 47.95 Da) but they may originate from the variation of the sample e.g. differences in the surface topography at the measurement spot.

Conclusions

In this paper we have shown that it is possible to form permanent planar fluidic channels on a TiO_2 nanoparticle coated paperboard. We have previously demonstrated controlled wettability using the photocatalytic activity of TiO_2. Here, a simple water treatment step in between the UVA illumination and the heat treatment removes the TiO_2 nanoparticles from the UVA exposed channel leaving the channel permanently lower in hydrophobicity compared to an untreated counterpart. The first stage wetted and non-wetted channel structures have been characterized in detail using CA, FE-SEM, XPS, and ToF-SIMS. The first stage wetting prevents the recovery of surface superhydrophobicity, and thus the shelf lifetime of such fluidic channels is significantly improved.

The used LFS technique allows cost-effective, roll-to-roll deposition of nanoparticles on large area webs. In this work we have demonstrated simple 1 and 2 mm wide planar channels on paperboard that can easily be extended towards more complicated structures with a different design of the used photomask. We plan to return on this issue in a future communication. Hence, the results of this work show avenues towards low-cost planar fluidic point-of-care diagnostic devices that are recyclable, renewable, and easily disposable after use without any need for laboratories. Furthermore, such natural fibre based products promote both ecologically and economically sustainable development. We believe that such planar fluidic channels will find many applications in diagnostics in the future.

Acknowledgements

This work is supported by the Academy of Finland (grant no. 250 122, 256 263, and 283 054).

Literature

Aromaa, M., Arffman, A., Suhonen, H., Haapanen, J., Keskinen, J., Honkanen, M. Nikkanen, J.-P., Levänen, E., Messing, M.E., Deppert, K., Teisala, H., Tuominen, M., Kuusipalo, J., Stepien, M., Saarinen, J.J., Toivakka, M., Mäkelä, J.M., (2012): Atmospheric synthesis of superhydrophobic TiO_2 nanoparticle deposits in a single step using liquid flame spray, J. Aerosol. Sci. 52, 57-68.

Balu, B., Berry, A.D., Hess, D.W., Breedveld, V. (2009): Patterning of superhydrophobic paper to control mobility of micro-liter drops for two-dimensional lab-on-paper applications, Lab Chip 9(21), 3066-3075.

Barr, M. C., Rowehl, J. A., Lunt, R. R., Xu, J., Wang, A., Boyce, C. M., Im, S. G., Bulovic, V., Gleason, K. K. (2011): Direct monolithic integration of organic photovoltaic circuits on unmodified paper, Adv. Mater. 23(31), 3500-3505.

Bollström, R., Määttänen, A., Tobjörk, D., Ihalainen, P., Kaihovirta, N., Österbacka, R., Toivakka, M., Peltonen, J. (2009): A multilayer coated fiber-based substrate suitable for printed functionality, Org. Electron. 10(5), 1020–1023.

Deegan, R.D., Bkajin, O., Dupont T.F., Huber, G., Nagel, S.R., Witten, T.A. (1997): Capillary flow as the cause of ring stains from dried liquid drops, Nature 389(6653), 827-829.

Fobel, R., Kirby, A.E., Ng, A.H.C., Farnood, R.R., Wheeler, A.R. (2014): Paper microfluidics goes digital, Adv. Mater. 26(18), 2838-2843.

Fujishima, A., Rao, T. N. and Tryk, D. A. (2000): Titanium dioxide photocatalysis, J. Photochem. Photobiol. C, 1(1), 1-21.

Gnanappa, A. K., Papageorgiou, D. P., Gogolides, E., Tserepi, A., Papathanasiou, A.G., Boudouvis, A.G., (2012): Hierarchical, plasma nanotextured, robust superamphiphobic polymeric surfaces structurally stabilized through a wetting–drying cycle, Plasma Process. Polym. 9(3), 304-315.

Gross, K.A., Tikkanen, J., Keskinen, J., Pitkänen, V., Eerola, M., Siikamäki, R., Rajala, M. (1999): Liquid flame spraying for glass coloring, J. Therm. Spray Technol. 8(4), 583-589.

Gunawan, C., Teoh, W.Y., Marquis, C.P., Lifia, J., Amal, R. (2009): Reversible antimicrobial photoswitching in nanosilver, Small 5(3), 341-344.

Hubbe, M.A. (2007): Paper's resistance to wetting - A review of internal sizing chemicals and their effects, BioRes. 2(1), 106–145.

Hübler, A., Trnovec, B., Zillger, T., Ali, M., Wetzold, N., Mingebach, M., Wagenpfahl, A., Deibel, C., Dyakonov, V. (2011): Printed paper photovoltaic cells, Adv. Energy Mater. 1(6), 1018-1022.

Irimia-Vladu, M., Glowacki, E.D., Voss, G., Bauer, S., Sariciftci, N.S. (2012): Green and biodegradable electronics, Mater. Today 15(7), 340–346.

Keskinen, H., Mäkelä, J.M., Aromaa, M., Keskinen, J., Areva, S., Teixeira, C.V., Rosenholm, J., Pore, V., Ritala, M., Leskelä, M., Raulio, M., Salkinoja-Salonen, M.S., Levänen, E., Mäntylä, T. (2006): Titania and titania-silver nanoparticle deposits made by liquid flame spray and their functionality as photocatalyst for organic- and biofilm removal, Catal. Lett. 111(3-4), 127–132.

Martinez, A.W., Phillips, S.T., Whitesides, G.M. (2008): Three-dimensional microfluidic devices fabricated in layered paper and tape, Proc. Nat. Acad. Sci. 105(50), 19606-19611.

Martinez, A.W., Phillips, S.T., Whitesides, G.M., Carrilho, E. (2010): Diagnostics for the developing world: Microfluidic paper-based analytical devices, Anal. Chem. 82(1), 3-10.

Mäkelä, J.M., Keskinen, H., Forsblom, T., Keskinen, J. (2004): Generation of metal and metal oxide nanoparticles by liquid flame spray process, J. Mater. Sci. 39(8), 2783–2788.

Mäkelä, J.M., Hellsten, S., Silvonen, J., Vippola, M., Levänen, E., Mäntylä, T., (2006): Collection of liquid flame spray generated TiO_2 nanoparticles on stainless steel surface, Mater. Lett. 60(4), 530-534.

Mäkelä, J.M., Aromaa, M., Teisala, H., Tuominen, M., Stepien, M., Saarinen, J.J., Toivakka, M., Kuusipalo, J. (2011): Nanoparticle deposition from liquid flame spray onto moving roll-to-roll paperboard material, Aerosol Sci. Technol. 45(7), 817-827.

Pelton, R. (2009): Bioactive paper provides a low-cost platform for diagnostics, Trends Anal. Chem. 28(8), 925–942.

Sarfraz, J., Määttänen, A., Ihalainen, P., Keppeler, M., Linden, M., Peltonen, J. (2012): Printed copper acetate based H_2S sensor on paper substrate, Sensor Actuat. B: Chemical 173, 868-873.

Siegel, A.C., Phillips, S.T., Wiley, B.J. and Whitesides, G.M. (2009): Thin, lightweight, foldable thermochromic displays on paper, Lab Chip 9(19), 2775–2781.

Songok, J., Tuominen, M., Teisala, H., Haapanen, J., Mäkelä, J., Kuusipalo, J., Toivakka, M. (2014): Paper-based microfluidics: Fabrication technique and dynamics of capillary-driven surface flow, ACS Appl. Mater. Interfaces 6(22), 20060-20066.

Stepien, M., Saarinen, J.J., Teisala, H., Tuominen, M., Aromaa, M., Kuusipalo, J., Mäkelä, J.M., Toivakka, M. (2011): Adjustable wettability of paperboard by liquid flame spray nanoparticle deposition, Appl. Surf. Sci. 257(6), 1911-1917.

Stepien, M., Saarinen, J.J., Teisala, H., Tuominen, M., Aromaa, M., Kuusipalo, J., Mäkelä, J.M., Toivakka, M. (2012): Surface chemical analysis of photocatalytic wettability conversion of TiO_2 nanoparticle coating, Surf. Coat. Technol. 208, 73-79.

Stepien, M., Saarinen, J.J., Teisala, H., Tuominen, M., Aromaa, M., Haapanen, J., Kuusipalo, J., Mäkelä, J.M., Toivakka, M. (2013): ToF-SIMS analysis of UV-switchable TiO_2-nanoparticle-coated paper surface, Langmuir 29(11), 3780-3790.

Takeda, S., Fukawa, M., Hayashi, Y., Matsumoto, K. (1999): Surface OH group governing adsorption properties of metal oxide films, Thin Solid Films 339(1), 220-224.

Teisala, H., Tuominen, M., Stepien, M., Haapanen, J., Mäkelä, J.M., Saarinen, J.J., Toivakka, M., Kuusipalo, J. (2013): Wettability conversion on the liquid flame spray generated superhydrophobic TiO_2 nanoparticle coating on paper and board by photocatalytic decomposition of spontaneously accumulated carbonaceous overlayer, Cellulose 20(1), 391-408.

Tobjörk, D., Österbacka, R. (2011): Paper electronics, Adv. Mater. 23(17), 1935–1961.

Vella, S.J., Beattie, P., Cademartini, R., Laromaine, A., Martinez, A.W., Phillips, S.T., Mirica, K.A., Whitesides, G.M. (2012): Measuring markers of liver function using a micropatterned paper device designed for blood from a fingerstick, Anal. Chem. 84(6), 2883-2891.

Whitesides, G.M. (2006): The origins and the future of microfluidics, Nature 442(7101), 368–373.

Manuscript received December 21, 2015
Accepted for publication April 21, 2016